# Low-Impedance Probes for Wireless Monitoring of Neural Activation

Carolina Moncion, Satheesh Bojja-Venkatakrishnan, Jorge Riera Diaz, John L. Volakis College of Engineering and Computing, Florida International University, Miami, FL e-mail: cmonc007@fiu.edu

Abstract — To address the need for high-quality brain monitoring, implantable systems are often used. However, these systems require significantly invasive procedures. This paper presents the development of probes specific to a device that can be used to record neural data during normal day-to-day activity. Here, the design of low-impedance neural probes for a fully-passive wireless brain implant is introduced and employed in a series of in vitro experiments. The integration of these neural probes to the neurosensing system results in enhanced impedance matching. As a result, neural signals as low as 15  $\mu Vpp$  can be detected with an RF sensitivity of  $\sim$  -135 dBm. This implies that the neurosensing system can record all neural activity measurable at the cortical surface.

Index Terms – Biomedical Telemetry, Electroencephalography, Impedance Matching, Implants, Neuroscience

#### I. INTRODUCTION

Electroencephalogram (EEG) refers to the recording of neural activation at the scalp [1]. As such, it depicts activity integrated over an area of the cerebral cortex and it is attenuated by the soft and hard tissues that protect the brain [1, 2]. Electrocorticograms (ECoG), on the other hand, have probes placed on the cortical surface thereby omitting the attenuating properties of the skull and protective tissues [1]. These signals have amplitudes in the µVpp scale with frequencies ranging from 1 Hz to several hundred hertz and even kilohertz in the case of local field potentials and spiking [1]. Cortical recordings are paired with complications, mostly stemming from their invasiveness. In addition, the current technology employs protruding wires, which are a source of infections and often limit studies to a clinical setting. Implanted neural recording systems can be designed without external connections, but they use power sources or batteries that can generate heat and require replacements [3, 4]. A fully-passive wireless brain implant, like the neurosensing system included in this paper, would overcome these shortcomings [3, 4].

A crucial feature of a biopotential acquisition system is the probe. This functions as a transducer, converting biological ionic currents into electric current that can be recorded [2]. In this case, the design and development of improved neural probe are motivated by the low input impedance of the neurosensing implant. Contrarily, modern biopotential monitoring systems have an input impedance in the order of  $10 \text{ M}\Omega$  [5]. To achieve effective signal transfer, the system's impedance is matched to their probes [5]. Consequently, high impedance probes matched to typical bipotential acquisition systems, are mismatched with the neurosensing implant.

Designing probes for devices with low input impedance, like the neurosensing system, is undoubtedly challenging. There are

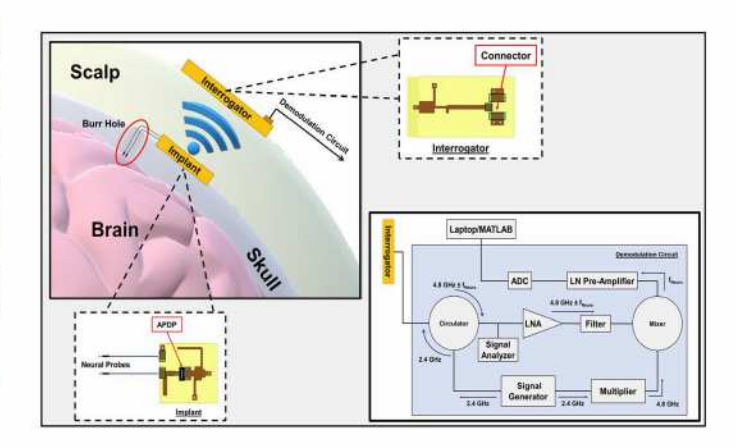


Fig. 1. Block diagram of the neurosensing system able to detect neural signals as low as 15  $\mu$ Vpp.

many factors to consider, as the electrical characteristics of the probes are affected by several physical properties [2]. In addition, there are physiological parameters to consider, such as spatial resolution [2, 6]. However, considering these attributes, we developed a probe multiple orders of magnitude lower than probes for analogous applications [7]. Coupling our probe with the neurosensing system led to neural detections as low as 15  $\mu$ Vpp. In addition to an RF sensitivity of  $\sim$  -135 dBm compared to other implantable neural systems with a sensitivity of  $\sim$ -77.7 dBm [4]. Such a neurosystem has a wide range of applications. To name a few, epilepsy and Alzheimer's progression analysis, as well as, the development of brain-computer interface technology for neurorehabilitation and prosthesis control.

In this paper, we present design considerations for low impedance neural probes, in addition to their testing. These probes help validate the enhanced sensitivity of the neurosensing system. Further, using the probes we demonstrate the system's capability of measuring neurosignals as low as 15  $\mu$ Vpp with maximal preservation of signal integrity.

## II. NEUROSENSING SYSTEM

The neurosensing system is comprised of three major components, the implant antenna, the interrogator antenna and the neural probes. As Fig. 1 depicts, the implant antenna is designed to be placed below the scalp while the interrogator antenna remains above the scalp. Furthermore, the neural probes encounter the cortical surface through an opening in the skull, namely a burr hole, as highlighted in Fig. 1. In addition, Fig. 1 includes a representation of the employed

filtering, amplification and demodulation circuit for extracting the neural signal.

## A. Implant and Interrogator Antenna

Using dual-band antenna, the neurosensing system was designed to radiate at 2.4 and 4.8 GHz  $\pm$   $f_{\text{neuro}}$  [3]. As Fig. 1 illustrates, to initiate and maintain monitoring an RF source, like a vector signal generator, is used to supply the interrogator with a 2.4 GHz carrier signal, which it transmits to the implant. Upon receiving this signal, the implant performs harmonic mixing, with minimal conversion loss, in its anti-parallel diode pair (APDP) to generate 4.8 GHz  $\pm$   $f_{\text{neuro}}$ , where  $f_{\text{neuro}}$  denotes the neural activation sensed by the probes. This modulated signal is retransmitted to the interrogator where it can be demodulated and analyzed.

# B. Neural Probes

An impedance characterization of the implant revealed that the input impedance varies with frequency from 5 Hz to a few hundred Hz. As seen in the inset of Fig. 2, the input impedance is approximately 2 k $\Omega$  for signals of frequency ~250 Hz compared to the 10 M $\Omega$  impedance of typical systems [5]. This paper focuses on presenting neural probes with lowered impedance magnitude and therefore enhanced impedance matching properties with the neurosensing system. As presented in [2], there are several properties related to geometry and material, that have a corresponding effect on the probe impedance. These properties include surface area and polarization.

Probe surface area is inversely proportional to the impedance. Two probes of the same material (Ag/AgCl) but different diameters (1.00 mm and ~0.3 mm) exhibit as much as a five-fold increase in impedance magnitude, especially at low frequencies. This behavior is depicted in Fig. 2. Intuitively, increasing the probe surface area until our desired impedance is achieved would be the appropriate course of action. However, this affects the sensitivity of the probe at the

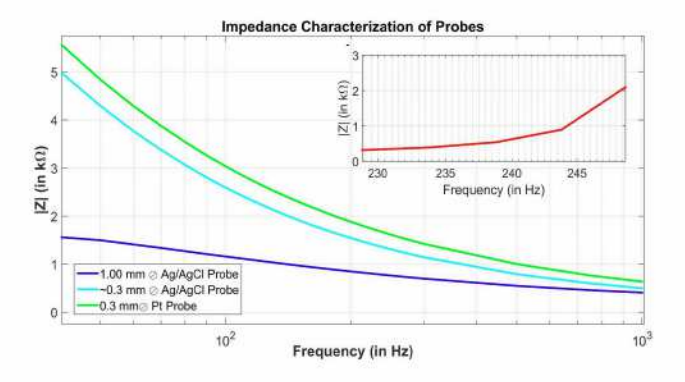


Fig. 2. Impedance characterization of the neural probes showing the effects of surface area and polarization variations. The inset shows an impedance characterization of the implant antenna ( $\sim 2~k\Omega$  at 250 Hz). Ag/AgCl: Silver-Silver Chloride. Pt. Platinum.

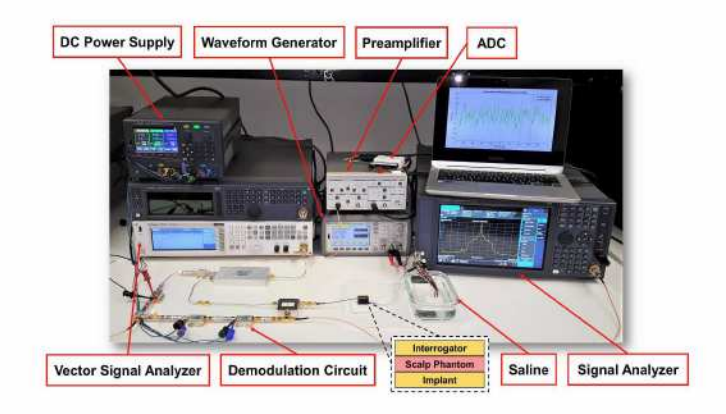


Fig. 3. In vitro experimental set-up used to evaluate the neurosensing system with the developed neural probes.

neural nodes and limits the range of neural activity that can be recorded [2]. For example, increasing the surface area also increases the area of neural activity that is sensed at a time [1]. This means the sensed neural signal is composed of a greater integrated cortical area. As a result, waveforms like local field potentials (LFPs), that depend on the number of sources, can become indiscernible [1].

Polarization properties are another factor affecting the probe impedance seen by the implant. At low frequencies, probe polarity increase impedance [2]. Ag/AgCl electrodes depict properties close to perfectly nonpolarized electrodes, making them practical for biomedical applications [2]. On the other hand, platinum (Pt) electrodes are highly polarized [2]. Fig. 2 highlights the effect of changing a Ag/AgCl probe to a Pt probe using an equivalent diameter, i.e. maintaining surface area constant.

Considering the above factors and their influence on probe impedance, we designed a bio-compatible neural probe to match the impedance of the implant (see inset of Fig. 2). At the same time, the probe remains minimally invasive to achieve maximum spatial resolution at the cortical surface [6].

## III. EXPERIMENTAL SET-UP

Our initial experimental set-up was based on the system shown in Fig. 1, without the neural probes. Sinusoidal single-frequency representatives of brain signals were generated using a waveform generator and provided to the implant for detection. We placed a phantom for the scalp layer (~2 mm in thickness) between the implant and interrogator antenna to simulate the implant being placed below the skin (see. Fig. 1). Then, the recovered signal was demodulated, amplified (10 – 100 dB gain) and recorded using a 12-bit ADC, as shown in Fig. 1. To evaluate sensitivity and modulated signal transmission between the antennas in a perfectly matched situation, the neural signal amplitude was gradually reduced and the frequency varied.

To address the need for a more realistic scenario, we designed an *in vitro* experimental set-up with the phantom for

the scalp layer and incorporating a physiological (0.9%) saline solution as a phantom for the brain (see Fig. 3). Single-frequency waveforms and signals with the characteristics of authentic multi-frequency spontaneous neural activation were induced in the solution, using a waveform generator, to simulate a clinical recording at the cortical surface. Doing so, it was possible to account for the interface between the implant and the neural probes in a medium that mimics the conductive properties of the brain. Thus, testing the effects of varying degrees of impedance mismatch between the probes and implant. The rest of the system, including the demodulation circuit, implant, and the interrogator, remained the same.

#### IV. MEASUREMENTS

Fig. 2 displays an impedance characterization of three of the developed probes, along with a focused characterization of the neurosensing implant. At ~250 Hz the impedance of the implant is ~2 k $\Omega$ , whereas the impedance of the Pt probe, for example, at this frequency is ~1.6 k $\Omega$ . This suggests that at this frequency there is a close to perfect match with the system. In addition, at other frequencies, the developed probes exhibit a closer match to the system than typical probes.

The measurements displayed in Table I indicate that the neurosensing system can detect sinusoidal signals with an amplitude as low as 15  $\mu$ Vpp across several frequencies, given an appropriately matched scenario. Furthermore, these measurements also express that the system can detect a modulated signal power (4.8 GHz  $\pm$  f<sub>neuro</sub>) as low as -132 dBm at low frequencies like 50 Hz and -129 dBm at higher frequencies up to 1 kHz.

Fig. 4 shows that simulating an authentic spontaneous EEG signal generated by a waveform generator can be sensed with the neurosensing system and demodulated with minimal signal distortion. A correlation analysis between the simulated and recovered neural signal resulted in a correlation coefficient of  $0.9346 \pm 0.0200$ . This also confirms the neurosensing system's ability to detect realistic multi-frequency neural signals with amplitude as low as 15  $\mu$ Vpp. The *in vivo* stage of this project will involve a series of experiments using the neurosensing system, including the low-impedance probes, to record neural activation in rats.

TABLE I

DETECTED MODULATED NEURAL SIGNAL POWER

Input Amplitude	Input Frequency		
	50 Hz	500 Hz	1 kHz
50 μ <b>V</b> pp	-119 dBm	-118 dBm	-118 dBm
40 μ <b>V</b> pp	- 120 dBm	-120 dBm	-120 dBm
30 μ <b>V</b> pp	-122 dBm	-123 dBm	-123 dBm
20 μVpp	-130 dBm	-128 dBm	-128 dBm
15 μVpp	-132 dBm	-129 dBm	-129 dBm

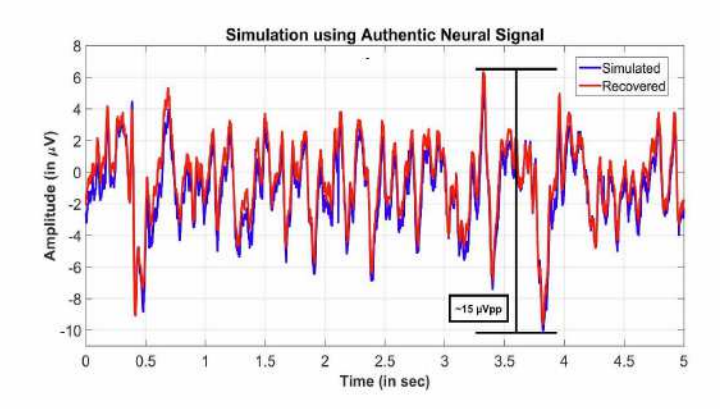


Fig. 4. Overlay of simulated and recovered (corrected for pre-amplifier gain) neural signal demonstrating the neurosensing system's capability to record signals as low as 15 μVpp.

#### V. CONCLUSIONS

For the first time, low impedance probes designed to improve impedance matching with the neurosensing system was presented and tested. Particularly, we presented two essential design considerations of neural probes, their development, and application in a brain phantom experiment. Measurements showed a system RF sensitivity down to approximately -135 dBm. Both single- and multi-frequency neural signals with amplitude as low as 15  $\mu$ Vpp were used in the simulation, an amplitude smaller than previously reported in [3], indicating the system can detect even minute neural signals. The demonstrated enhanced performance of this system ensures the ability to record the broad spectrum of neural signals generated by the brain. At the conference, we will present results from a series of *in vivo* rat experiments.

## REFERENCES

- G. Buzsáki, C. A. Anastassiou, and C. Koch, "The origin of extracellular fields and currents-EEG, ECoG, LFP and spikes," *Nat. Rev. Neurosci.*, vol. 13, no. 6, pp. 407–420, 2012.
- [2] E. J. D. Bronzino, "Neuman, M. R. 'Biopotential Electrodes.," Med. Instrum. Appl. Des., p. 713, 2010.
- [3] C. W. L. Lee, A. Kiourti, and J. L. Volakis, "Miniaturized Fully Passive Brain Implant for Wireless Neuropotential Acquisition," *IEEE Antennas Wirel. Propag. Lett.*, vol. 16, pp. 645–648, 2017.
- [4] Ming Yin, D. A. Borton, J. Aceros, W. R. Patterson, and A. V. Nurmikko, "A 100-Channel Hermetically Sealed Implantable Device for Chronic Wireless Neurosensing Applications," *IEEE Trans. Biomed. Circuits Syst.*, vol. 7, no. 2, pp. 115–128, Apr. 2013.
- [5] M. R. Neuman, "Biopotential amplifiers," Biomed. Eng. (NY)., no. 2, pp. 241–292, 2000.
- [6] B. Wodlinger, A. D. Degenhart, J. L. Collinger, E. C. Tyler-Kabara, and W. Wang, "The impact of electrode characteristics on electrocorticography (ECoG)," Proc. Annu. Int. Conf. IEEE Eng. Med. Biol. Soc. EMBS, vol. c, no. 1, pp. 3083–3086, 2011.
- [7] C. M. Lin, Y. T. Lee, S. R. Yeh, and W. Fang, "Flexible Carbon Nanotubes Electrode for Neural Recording," *Biosens. Bioelectron.*, vol. 24, no. 9, pp. 2791–2797, 2009.